05,11

Influence of Ga-substitution to the structural and magnetic properties of (Mn,Fe)$_2$O$_3$ bixbyite

© *E.M. Moshkina*[1], *M.S. Molokeev*[1,2,3], *E.V. Eremin*[1,2,4], *L.N. Bezmaternykh*[1]

[1] Kirensky Institute of Physics, Federal Research Center KSC SB, Russian Academy of Sciences,
Krasnoyarsk, Russia
[2] Siberian Federal University,
Krasnoyarsk, Russia
[3] Far Eastern State Transport University,
Khabarovsk, Russia
[4] Siberian State University of Science and Technology,
Krasnoyarsk, Russia

E-mail: ekoles@iph.krasn.ru

To study the dependence of the properties of ternary oxides (Mn,Fe,Ga)$_2$O$_3$ with the bixbyite structure on the composition, the temperature dependences of the magnetization and ac magnetic susceptibility of two single-crystal samples of different compositions obtained using the flux method were analyzed. A detailed study of the structure was carried out using single-crystal X-ray diffraction analysis, and the changes in structural parameters depending on the composition were analyzed. The dc magnetization and ac magnetic susceptibility of Fe$_{1.1}$Mn$_{0.76}$Ga$_{0.14}$O$_3$ and Fe$_{0.65}$Mn$_{1.1}$Ga$_{0.26}$O$_3$ bixbyites have been studied. Despite the qualitatively similar behavior of the magnetic properties, significant differences were also found, despite a small difference in the Mn/Fe/Ga ratio in the samples under study. It is shown that both compounds experience two successive low-temperature magnetic phase transitions from the paramagnetic phase at $T = 20-32$ K as the temperature is lowered. Calculations of the Mydosh parameter for the detected phase transitions showed different degrees of ordering in the compounds under study.

Keywords: transition metal oxides, magnetic phase transitions, spin glass state, bixbyite.

DOI: 10.21883/PSS.2023.06.56116.57

1. Introduction

At this point, transition metal oxides are a widely investigated class of compounds with detailed phase diagrams of binary and many ternary systems [1–4]. MnFeO$_3$ bixbyite isostructural to β-Mn$_2$O$_3$ is not an exception — it has been known for more than half a century already and there are numerous studies devoted to the properties of this compound [1–9]. However, some uncertainty of magnetic properties of MnFeO$_3$ is observed depending on the preparation method. According to some data, MnFeO$_3$ becomes ferrimagnetic at room temperature already and undergoes transition to the antiferromagnetic state at $T_N = 35$ K [5,6]. According to other data, only low-temperature phase transition occurs at T about $30-40$ K into a partially ordered phase with the spin glass state [7]. This discrepancy may be attributed to different distribution of iron and manganese cations over nonequivalent positions and to cation fraction valency variation [8]. Moreover, properties of MnFeO$_3$ may change as a result of high-temperature annealing [3].

This study investigates single-crystal samples of (Mn,Fe,Ga)$_2$O$_3$ ternary system prepared by flux method from fluxes with different Mn/Fe/Ga ratio using the same

temperature specifications. Thus, dependence of properties on composition of Ga-substituted bixbyites with similar preparation conditions is studied.

2. Experimental conditions

Fe$_{1.1}$Mn$_{0.76}$Ga$_{0.14}$O$_3$ and Fe$_{0.65}$Mn$_{1.1}$Ga$_{0.26}$O$_3$ single-crystal samples (composition is based on the energy-dispersive spectroscopy (EDX) data) were prepared using the flux method. The growth procedure is described in detail in [9].

Radiographic tests of Fe$_{1.1}$Mn$_{0.76}$Ga$_{0.14}$O$_3$ and Fe$_{0.65}$Mn$_{1.1}$Ga$_{0.26}$O$_3$ samples were carried out at room temperature 296(2) K using SMART APEX II single crystal diffractometer (the data was obtained using equipment provided by Krasnoyarsk Regional Common Use Center, Federal Research Center of Krasnoyarsk Science Center of Siberian Branch of RAS) using monochromatized Mo$K\alpha$ radiation, $\lambda = 0.7106$ Å. orientation matrix and cell parameters were determined and updated for all 2840 and 8617 reflections, respectively. The cells corresponded to cubic crystal system, sp. gr. $Ia\bar{3}$. Absorption correction of intensities is introduced in SADABS software. Basic

Table 1. Basic crystallographic characteristics and experiment parameters

	$Fe_{0.65}Mn_{1.1}Ga_{0.26}O_3$	$Fe_{1.1}Mn_{0.76}Ga_{0.14}O_3$
Chemical formula	$(Fe,Ga,Mn)_{16}O_{24}$	$(Fe,Ga,Mn)_{16}O_{24}$
Temperature (K)	296(2)	296(2)
Space group, Z	$Ia\bar{3}$, 2	$Ia\bar{3}$, 2
a (Å)	9.4106(6)	9.4108(3)
V (Å^3)	833.40(16)	833.45(8)
ρ_{calc} (g/cm^3)	5.033	5.033
μ (mm^{-1})	11.783	11.782
Number of measured reflections	2840	8617
Number of independent reflections	387	408
Number of strong reflections	375	375
$F > 4\sigma(F)$		
$2\theta_{max}$ (°)	77.71	78.042
h, k, l — limits	$-9 \le h \le 16;$	$-16 \le h \le 16;$
	$-12 \le k \le 16;$	$-16 \le k \le 16;$
	$-10 \le l \le 10$	$-16 \le l \le 16$
R_{int}	0.0393	0.0658
Updated results		
weighting scheme	$w = 1/[\sigma^2(F_o^2) + (0.1000P)^2]$	$w = 1/[\sigma^2(F_o^2) + (0.0284P)^2 + 2.7030P]$
	where $P = \max(F_o^2 + 2F_c^2)/3$	where $P = \max(F_o^2 + 2F_c^2)/3$
Number of parameters to be updated	18	18
$R1[F_o > 4\sigma(F_o)]$	0.0270	0.0206
$wR2$	0.1088	0.0487
Goof	1.026	1.084
$\Delta\rho_{max}$ (e/Å^3)	1.523	0.857
$\Delta\rho_{min}$ (e/Å^3)	-0.839	-0.831
$(\Delta/\sigma)_{max}$	< 0.001	< 0.001
Extinction coefficient	0.019(4)	0.0246(12)

crystallographic characteristics and experiment acquisition parameters are listed in Table 1. Simulation was carried out in SHELXT software [10] by direct methods. As a result, coordinates of all atoms were found. The resulting structure was updated using thermal parameter anisotropy of all atoms by the least-square method.

Dependences of magnetization on temperature and field and dependences of magnetic susceptibility on temperature ac were obtained within $4.2-300$ K and in magnetic fields up to 9 T using PPMS-9 (Quantum Design) system.

3. Structural properties of (Mn,Fe,Ga)$_2$O$_3$ bixbyites

Main crystallographic characteristics of the test samples and experiment acquisition parameters are listed in Table 1, main bond lengths are listed in Table 2. As expected, the studied compounds are isostructural equivalents of FeMnO$_3$ and β-Mn$_2$O$_3$ with bixbyite structure with some differences in crystallographic parameters caused by different cation composition. They have space group $Ia\bar{3}$, lattice cell contains two non-equivalent cation positions in the octahedral oxygen atom environment (Figure 1). For comparison, Table 2 shows bond lengths of three $Fe_{2-x}Mn_xO_3$ solid

solutions [11–12]. Data in Table 2 is listed in ascending order of iron content.

The lattice constants of the test oxides are rather similar, however, the bond lengths in the oxygen octahedron of position $M2$ are different. Unlike the oxygen environment of position $M1$ that has an undistorted ideal octahedron symmetry, the octahedral environment of cation in position $M2$ is characterized by rhombic symmetry C_{2v}: the octahedron is extended and slightly compressed in the orthogonal plane. Such type of octahedral distortion is typical for $Mn^{3+}-O$ octahedra as structural components due to the Jahn-Teller effect [13]. Actually, with decreasing manganese content, the „long" bond in $M2$-O octahedron also decreases. An interesting feature includes the proximity of bond lengths of $Fe_{1.1}Mn_{0.76}Ga_{0.14}O_3$ and $Fe_{1.26}Mn_{0.7}4O_3$ [11] with almost equal manganese content. Thus, the structural parameter variation in these compounds is primarily defined by the content of Mn^{3+}.

4. Magnetic properties of (Mn,Fe,Ga)$_2$O$_3$ bixbyites

Dependences of magnetization on temperature for $Fe_{1.1}Mn_{0.76}Ga_{0.14}O_3$ and $Fe_{0.65}Mn_{1.1}Ga_{0.26}O_3$ single-crystals obtained at $H = 1$ kOe $(H \parallel a)$ are shown in

Table 2. Main bond lengths

	Fe$_{0.034}$Mn$_{1.966}$O$_3$ [11]	Fe$_{0.65}$Mn$_{1.1}$Ga$_{0.26}$O$_3$	FeMnO$_3$ [12]	Fe$_{1.1}$Mn$_{0.76}$Ga$_{0.14}$O$_3$	Fe$_{1.26}$Mn$_{0.74}$O$_3$ [11]
$M1-$O^{i}	2.0032	**2.0036(17)**	2.0132	**2.0121(12)**	2.0090
$M1-$O^{iii}	2.0032	**2.0036(17)**	2.0132	**2.0121(12)**	2.0090
$M1-$O^{v}	2.0032	**2.0036(17)**	2.0132	**2.0121(12)**	2.0090
$M1-$O^{ii}	2.0032	**2.0036(17)**	2.0132	**2.0121(12)**	2.0090
$M1-$O^{iv}	2.0032	**2.0036(17)**	2.0132	**2.0121(12)**	2.0090
$M1-$O	2.0032	**2.0036(17)**	2.0132	**2.0121(12)**	2.0090
$M2-$O	1.8975	**1.9153(18)**	1.9134	**1.9305(13)**	1.9302
$M2-$O^{xiii}	1.9870	**2.0149(19)**	1.9243	**2.0341(13)**	2.0325
$M2-$O^{xv}	2.2423	**2.1859(19)**	2.2433	**2.1399(14)**	2.1466
$M2-$O^{xii}	1.8975	**1.9154(18)**	1.9134	**1.9306(13)**	1.9302
$M2-$O^{xiv}	1.9870	**2.0149(19)**	1.9243	**2.0341(13)**	2.0325
$M-$O^{xvi}	2.2423	**2.1859(19)**	2.2433	**2.1399(14)**	2.1466

N o t e. Symmetry elements: (i) $-y + 3/2, -z + 3/2, -x + 3/2$; (ii) , , ; (iii) $-x + 3/2, -y + 3/2, -z + 3/2$; (iv) , , ; (v) $-z + 3/2, -x + 3/2, -y + 3/2$; (vi) $-x + 1, -y + 3/2, z$; (vii) $-z + 1, x, y + 1/2$; (viii) $z, -x + 3/2, y + 1/2$; (ix) $y + 1/2, -z + 3/2, -x + 1$; (x) $-y + 3/2, z, -x + 1$.
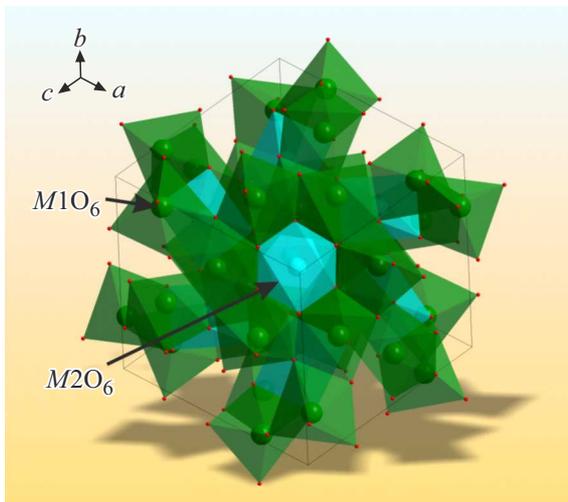

Figure 1. Bixbyite structure. Oxygen octahedra corresponding to non-equivalent cation positions $M1$ and $M2$, respectively, are shown in blue and green color.

Figure 2. Measurements were performed in three modes: ZFC — sample heating in non-zero magnetic field after pre-heating in zero magnetic field; FC — sample cooldown in non-zero magnetic field; FH — sample heating in non-zero magnetic field after pre-cooling in magnetic field of the same strength. In Figure 2, *1* and *2* denote groups of curves of the corresponding Fe$_{1.1}$Mn$_{0.76}$Ga$_{0.14}$O$_3$ and Fe$_{0.65}$Mn$_{1.1}$Ga$_{0.26}$O$_3$ bixbyites.

As can be seen from Figure 2, magnetization of both test compounds behaves similarly: gradual ascent and sharp maximum occur in the low temperature region corresponding to the magnetic phase transition. Below the phase transition temperature, magnetization decreases and bifurcation of FC and ZFC curves is observed. Dependences obtained in FC and FH conditions are almost coincident. However, for both compounds, there is a minor difference

in these curves obtained in sample heating and cooling conditions, and this may be indicative of a temperature dependence — presence of spin glass sate. Significant difference in curves FC and ZFC is indicative of potential presence of spin glass state.

Temperature behavior of magnetization of Fe$_{1.1}$Mn$_{0.76}$Ga$_{0.14}$O$_3$ and Fe$_{0.65}$Mn$_{1.1}$Ga$_{0.26}$O$_3$ is qualitatively similar. However, in the low-temperature phase, magnetization of the sample with lower manganese content remains constant at a temperature up to $T = 15$ K, and the sample with high manganese content has magnetization minimum with corresponding ascent at low temperatures. Similar behavior may be associated with paramagnetic
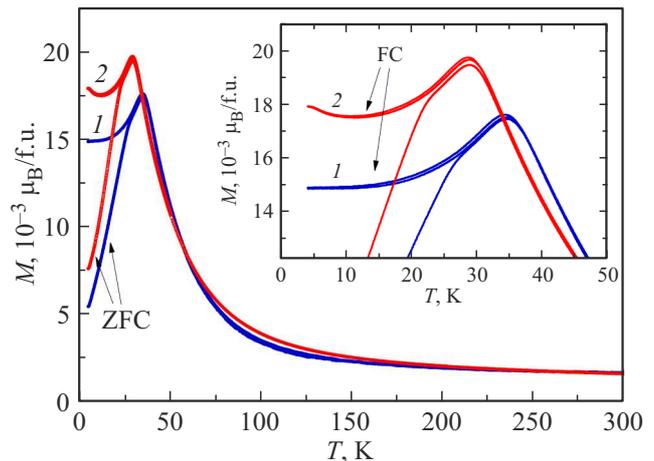

Figure 2. Dependences of magnetization on temperature for Fe$_{1.1}$Mn$_{0.76}$Ga$_{0.14}$O$_3$ (*1*) and Fe$_{0.65}$Mn$_{1.1}$Ga$_{0.26}$O$_3$ (*2*) single-crystals obtained at $H = 1$ kOe ($H \parallel a$). Measurements were performed in three modes: ZFC — sample heating in non-zero magnetic field after pre-heating in zero magnetic field; FC — sample cooldown in non-zero magnetic field; FH — sample heating in non-zero magnetic field after pre-cooling in magnetic field of the same strength.
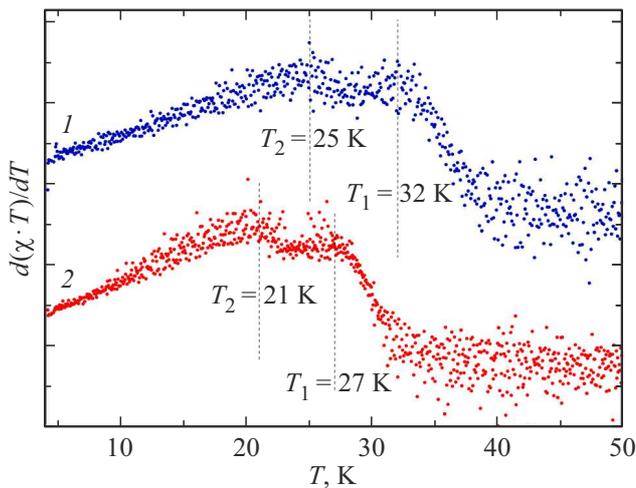
Figure 3. temperature dependences of derivatives $\partial(\chi T)/\partial T$ of $Fe_{1.1}Mn_{0.76}Ga_{0.14}O_3$ (1) and $Fe_{0.65}Mn_{1.1}Ga_{0.26}O_3$ bixbyites (2). Dependences of magnetization on temperature obtained in ZFC mode were used as input for calculation and plotting of these curves.

growth of magnetization as a result of partial ordering of magnetic moments [14].

According to early studies of magnetic properties of Mn−Fe bixbyites, this phase transition is classified as paramagnetic-antiferromagnetic transition. It is known that in collinear two-sublattice antiferromagnets, magnetic contribution to thermal capacity C_m is proportional to $\partial(\chi T)/\partial T$ [15]. Figure 3 shows dependences $\partial(\chi T)/\partial T(T)$ of the studied oxides. As can be seen in the Figure, this dependence in both compounds shows two peaks corresponding to two magnetic phase transitions at $T_1 = 32$ K and $T_2 = 25$ K for $Fe_{1.1}Mn_{0.76}Ga_{0.14}O_3$ and $T_1 = 27$ K and $T_2 = 21$ K for $Fe_{0.65}Mn_{1.1}Ga_{0.26}O_3$. Peak asymmetry of temperature dependence ZFC indicating that two, rather

than one, magnetic phase transitions take place is also shown in detail in Figure 2.

Field dependences of magnetization of both samples are shown in Figure 4. It can be seen that at $T = 4.2$ K (Figure 4, a), they qualitatively correspond to each other and look like extended unlimited loops with coercive fields 7.8 kOe and 5.7 kOe for $Fe_{1.1}Mn_{0.76}Ga_{0.14}O_3$ and $Fe_{0.65}Mn_{1.1}Ga_{0.26}O_3$, respectively. Figure 4, b shows field dependences of magnetization of $Fe_{1.1}Mn_{0.76}Ga_{0.14}O_3$ bixbyite obtained at different temperatures. As shown in the Figure, dependences at $T = 100$ K and $T = 150$ K are linear and correspond to paramagnetic state. Dependence obtained at $T = 50$ K near the phase transition temperature is not linear which is indicative of obvious influence of the near magnetic correlations at the temperature already.

For more detailed study of the detected magnetic phase transitions, temperature dependences ac of magnetic susceptibility of both compounds were obtained and analyzed. Curves obtained for real and imaginary part ac of magnetic susceptibility are shown in Figure 5. Dependences of the real part of both samples show sharp peak in the low-temperature region corresponding to magnetic phase transitions detected on the temperature dependences of magnetization. This maximum has a weakly asymmetrical shape which suggests the presence of at least two, rather than one, magnetic phase transitions. $Fe_{1.1}Mn_{0.76}Ga_{0.14}O_3$ sample (1) has an obvious frequency dependence of the detected peak position on the external magnetic field frequency. In the second sample, $Fe_{0.65}Mn_{1.1}Ga_{0.26}O_3$ (2), frequency dependence is much less pronounced. The temperature dependences of imaginary part ac of magnetic susceptibility have inflections corresponding to the temperatures of the maxima center position of the real part. There is a considerable dependence of the inflection position on the magnetic field frequency in the sample with lower manganese content, like in the real part. For this sample at
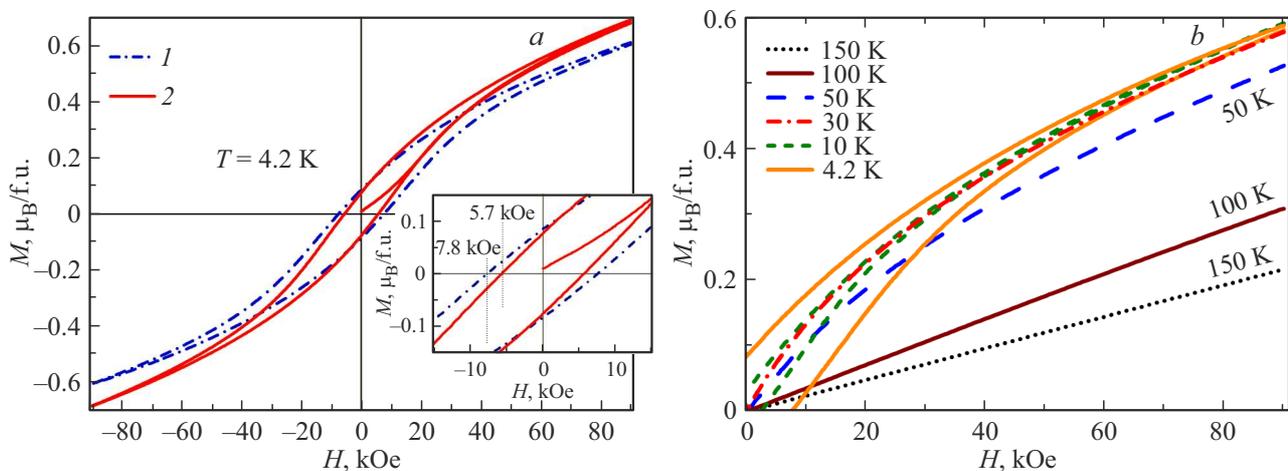

Figure 4. Field dependences of magnetization of $Fe_{1.1}Mn_{0.76}Ga_{0.14}O_3$ (1) and $Fe_{0.65}Mn_{1.1}Ga_{0.26}O_3$ (2) single-crystals. a — field dependences of $Fe_{1.1}Mn_{0.76}Ga_{0.14}O_3$ and $Fe_{0.65}Mn_{1.1}Ga_{0.26}O_3$, obtained at $T = 4.2$ K ($H \parallel a$). b — field dependences of $Fe_{1.1}Mn_{0.76}Ga_{0.14}O_3$ obtained at different temperatures with magnetic field applied along $H \parallel a$.

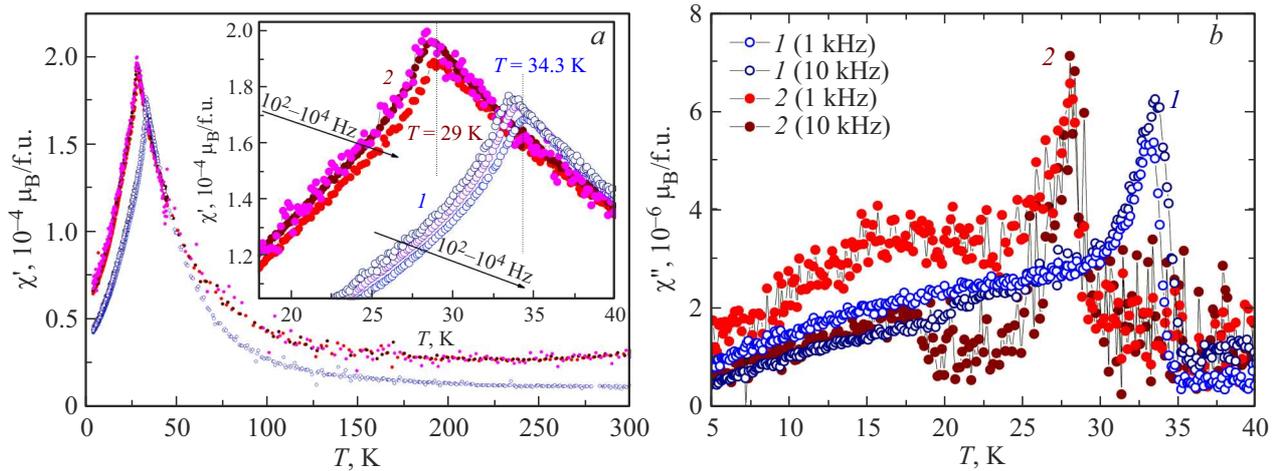**Figure 5.** temperature dependences ac of magnetic susceptibility of $Fe_{1.1}Mn_{0.76}Ga_{0.14}O_3$ (*1*) and $Fe_{0.65}Mn_{1.1}Ga_{0.26}O_3$ (*2*) bixbyites. *a* — temperature dependences of the real part; *b* — temperature dependences of imaginary part. Amplitude of external ac magnetic field 10 Oe. Measurements were carried out at external ac magnetic field frequency $f = 100, 1000, 10000\,Hz$.

temperatures below the inflection (*1*), wide declining „arm" is observed which probably corresponds to the second pgase transition. For the sample with high manganese content (*2*), a pronounced inflection corresponding to the real part peak center position is observed in the imaginary part. However, the amplitude of this inflection is considerably lower than in sample (*1*) and frequency dependence is absent. At low temperatures, low-intensity wide „arm" was detected on this curve. The shape of this arm varies with frequency. However, due to significant noise of the experimental points, analysis of this „arm" will be difficult. At temperatures of the second phase transition detected during the analysis of temperature dependences dc of sample magnetization (*1*), no imaginary part inflections were observed on the curve, which may be indicative of the antiferromagnetic origin of this transition.

Due to the obtained dependence of magnetic susceptibility peaks on frequency ac in the studied compounds, the Mydosh parameter, denoting whether spin-glass behavior is present in the samples, was calculated [16,17]:

$$\Omega = (T_2 - T_1)/\left(T_2 \cdot (\log \nu_2 - \log \nu_1)\right); \qquad (1)$$

where T_1 and T_2 are peak center position temperatures corresponding to frequencies ν_1 and ν_2. The calculation provided the Mydosh parameters equal to 0.0145 and 0.0007 for $Fe_{1.1}Mn_{0.76}Ga_{0.14}O_3$ (*1*) and $Fe_{0.65}Mn_{1.1}Ga_{0.26}O_3$ (*2*), respectively.

It is known [16,17] that the typical Mydosh parameter values for standard spin glasses are from 0.004 to 0.02 with higher values corresponding to cluster spin glasses. Thus, the bixbyite with lower manganese ion content has a spin glass state and the bixbyite with higher manganese ion content has magnetic phase transitions no related to „freesing" of magnetic moments. Nevertheless, the shown estimate is integral, because it does not consider

the presence of two magnetic phase transitions in each compound due to insufficient peak resolution.

5. Conclusion

Structural and magnetic properties of two Ga-substituted oxides $Fe_{1.1}Mn_{0.76}Ga_{0.14}O_3$ and $Fe_{0.65}Mn_{1.1}Ga_{0.26}O_3$ with bixbyite structure were studied. It is shown that structural parameters of the studied compounds, despite their different cation content, are very similar to each other and also agree with $Fe_{2-x}Mn_xO_3$ binary solid solutions that were studied before. The comparative analysis of the bond lengths of M2-O oxygen octahedron has shown that the main symmetry variations in it depend on the manganese ion concentration variation in the compound.

In the low-temperature region, two successive magnetic phase transitions were detected at $T_1 = 32\,K$ and $T_2 = 25\,K$ for $Fe_{1.1}Mn_{0.76}Ga_{0.14}O_3$ and $T_1 = 27\,K$ and $T_2 = 21\,K$ for $Fe_{0.65}Mn_{1.1}Ga_{0.26}O_3$. Magnetic properties of the studied bixbytes are similar in terms of quality, however, differences were detected that are associated with different degree of ordering: paramagnetic increase of magnetization in the low-temperature phase in oxide with higher manganese ion content and spin glass state in oxide with lower manganese ion content. Thus, the influence of cation content on the structural parameters and magnetic ordering in bixbyites was shown.

Federal Research Center of Krasnoyarsk Science Center of Siberian Branch of RAS.

Conflict of interest

The authors declare that they have no conflict of interest.

References

[1] B. Kholk, A. Albers, G.R. Hearne, H. Le Roux. Hyperfine Interact. **42**, 1051 (1988).

[2] Zhijie Li, Shifa Wang, Bo Li, Xia Xiang. J. Nano Res. **37**, 122 (2015).

[3] D. Seifu, A. Kebede, F.W. Oliver, E. Hoffman, E. Hammond, C. Wynter, A. Aning, L. Takacs, I.-L. Siu, J.C. Walker, G. Tessema, M.S. Seehra. J. Magn. Magn. Mater. **212**, 178 (2000).

[4] B.L. Sreenevas. Nature **181**, 864 (1958).

[5] S. Rayaprol, S.D. Kaushik, P.D. Babu, V. Siruguri. AIP Conf. Proc. **1512**, 1132 (2013).

[6] S. Rayaproln, S.D. Kaushik. Ceram. Int. **41**, *8*, 9567 (2015).

[7] Debamalya Ghosh, Uma Dutta, Ariful Haque, N.E. Mordvinova, O.I. Lebedev, Kamalesh Pal, Arup Gayen, Partha Mahata, Asish K. Kundu, Md. Motin Seikh. Mater. Sci. Eng. B **226**, 206, (2017).

[8] S. Rayaprol, Renan A.P. Ribeiro, Kiran Singh, V.R. Reddy, S.D. Kaushik, Sergio R. de Lazaro. J. Alloys Compd. **774**, 290 (2019).

[9] E. Moshkina, Yu. Seryotkin, O. Bayukov, M. Molokeev, D. Kokh, E. Smorodina, A. Krylov, L. Bezmaternykh. Cryst. Eng. Commun. (2015). In Press.

[10] G.M. Sheldrick. Acta Cryst. A. **64**, 112 (2008).

[11] S.Geller. Acta Crystallographica B **27**, 821 (1971).

[12] H. Dachs. Z. Kristallographie **107**, 370 (1956).

[13] E.M. Moshkina, N.A. Belskaya, M.S. Molokeev, A.F. Bovina, K.A. Shabanova, D. Kokh, Yu.V. Seretkin, D.A. Velikanov, E.V. Eremin, A.S. Krylov, L.N. Bezmaternykh. ZhETF **163**, *1*, 24 (2023). (in Russian)

[14] R.M. Eremina, T.P. Gavrilova, E.M. Moshkina, I.F. Gilmutdinov, R.G. Batulin, V.V. Gurzhiy, V. Grinenko, D.S. Inosov. J. Magn. Magn. Mater. **515**, 167262 (2020).

[15] E.E. Bragg, M.S. Seehra. Phys. Rev. B **7**, *9*, 4197 (1973).

[16] Sayandeep Ghosh, Deep Chandra Joshi, Prativa Pramanik, Suchit K. Jena, Suresh Pittala, Tapati Sarkar, Mohindar S. Seehra, Subhash Thota. J. Phys.: Condens. Matter **32**, 485806 (2020).

[17] Tapati Sarkar, V. Pralong, V. Caignaert, B. Raveau. Chem. Mater. **22**, 2885 (2010).

Translated by E.Ilyinskaya